

Theoretical Study of the Elimination Kinetics of Carboxylic Acid Derivatives in the Gas Phase. Decomposition of 2-Chloropropionic Acid

Vicent S. Safont,* Vicente Moliner, and Juan Andrés

Departament de Ciències Experimentals, Universitat Jaume I, Box 224, 12080 Castelló, Spain

Luís R. Domingo

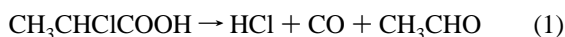
Departament de Química Orgànica, Universitat de València, Dr. Moliner 50, 46100 Burjassot, València, Spain

Received: August 16, 1996; In Final Form: January 2, 1997[⊗]

The reaction mechanism for the decomposition of 2-chloropropionic acid in the gas phase to form hydrogen chloride, carbon monoxide, and acetaldehyde has been theoretically characterized. Analytical gradients have been used by means of AM1 and PM3 semiempirical procedures and ab initio methods at HF and DFT (BLYP) levels with the 6-31G** basis set. The correlation effects were also included by using the perturbational approach at the MP2 level with the 6-31G** and 6-31++G** basis sets and the variational approach at the CISD/6-31G** level and by means of MCSCF wave functions with a (6,6) complete active space and the 6-31G** basis set. The global potential energy surface has been studied, and the stationary points were localized and characterized. The geometries, electronic structure, and transition vector associated with the transition structures have been analyzed and the dependence of these properties upon theoretical methods is discussed. The present study points out, in agreement with the experimental data, that the decomposition process occurs through a two-step mechanism involving the formation of the α -propiolactone intermediate. The transition structure associated with the first step can be described as a five-membered ring with participation of leaving chloride and hydrogen, assisted by the carbonyl oxygen of the carboxyl group. The second transition structure, controlling the α -propiolactone decomposition step, yields the formation of CO and CH₃CHO molecules. The rate constants and the Arrhenius preexponential factors for the different interconversion steps have been calculated in terms of the transition state theory. The comparison of experimental and theoretical values for these parameters allows us to prove the validity of theoretical methods. The results suggest that the process must be considered as essentially irreversible, the first step being the rate-determining step. From a computational point of view, the inclusion of the correlation energy at the MP2/6-31G** level is necessary to obtain an accurate calculation of the kinetic parameters.

Introduction

The kinetics of the gas phase decomposition of several carboxylic acid derivatives has been experimentally studied by Chuchani and co-workers.^{1–5} The results prove the reaction to be homogeneous, to be unimolecular, and to obey a first-order rate law. In particular, the rate coefficient for the gas phase decomposition of 2-chloropropionic acid (CH₃CHClCOOH) to form hydrogen chloride, carbon monoxide, and acetaldehyde



has been determined¹ at relatively low pressure and expressed as a function of temperature by the following Arrhenius-type equation:

$$\log k_{\text{obs}} (\text{s}^{-1}) = (12.53 \pm 0.43) - \frac{(186.9 \pm 5.1) \text{ kJ mol}^{-1}}{(2.303RT)} \quad (2)$$

There is an absence of theoretical studies on the nature of the molecular mechanism for this decomposition process. In this paper, the first of a series dealing with gas phase elimination kinetics of carboxylic acids derivatives, we have carried out theoretical calculations for the decomposition of 2-chloropropionic acid using several semiempirical and ab initio techniques. The aim of this work is to carry out a theoretical study with the

hope of addressing the experimental facts, to complement the extensive experimental data, and to illustrate the important interplay between experimental and theoretical efforts in the elucidation of such reactions. We hope to show how theory may contribute significantly to the unravelling of reaction mechanisms in cases experimentally unfeasible or at least very unattractive.

Computational Method and Model

All calculations have been performed with the GAUSSIAN92/DFT⁶ and GAUSSIAN94⁷ programs. The semiempirical calculations have been made by using the PM3^{8,9} and AM1¹⁰ methods, and the ab initio calculations were made at the HF/6-31G**¹¹ level. The correlation effects have been estimated by using the perturbational approach¹² at the MP2/6-31G** and MP2/6-31++G**¹³ levels and by using the variational approach at the CISD/6-31G**¹⁴ level. The density functional theory (DFT)^{15–18} has been employed with the Becke 1988 functional,¹⁹ which includes Slater exchange along with corrections involving the gradient of density, and the correlation functional of Lee, Yang, and Parr,^{20,21} which includes both the local and nonlocal terms, at the BLYP/6-31G** level. The inclusion of calculations based on DFT in the present study has the purpose of testing the ability of this methodology for describing the kinetics of processes like the one studied. DFT methods are computationally less expensive, and they take into account the electron correlation and thus can be, at least in principle, of comparable

* To whom correspondence should be addressed.

[⊗] Abstract published in *Advance ACS Abstracts*, February 15, 1997.

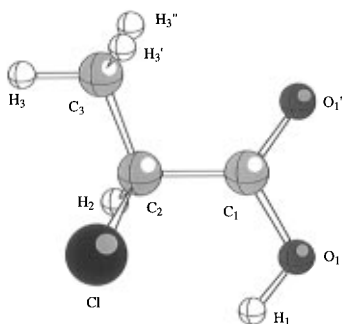


Figure 1. Atom numbering for 2-chloropropionic acid.

quality to the standard post-HF procedures. Finally, we have also performed calculations using MCSCF wave functions^{22–26} that contain the configurations corresponding to all possible occupancies of six orbitals by six electrons (corresponding to the bonds that are being broken/formed in the first step). These complete active space (CAS)SCF calculations have been carried out with the 6-31G** basis set, for the reactant and the first transition structure. The atom numbering for 2-chloropropionic acid is depicted in Figure 1.

The Bery analytical gradient optimization routines^{27,28} were used for optimization. The requested convergence on the density matrix was 10^{-9} atomic units, and the threshold value of maximum displacement was 0.0018 Å and that of maximum force was 0.000 45 hartree/bohr. The nature of each stationary point was established by calculating and diagonalizing the Hessian matrix (force constant matrix). An eigenvalue following algorithm²⁹ was used for locating the transition structures (TSs), which were characterized by means of a normal mode analysis, and the unique imaginary frequency associated with the transition vector (TV)³⁰ has been calculated. The intrinsic reaction coordinate (IRC)³¹ path has been traced in order to check and obtain energy profiles connecting each TS to the two associated minima of the proposed mechanism by using the second-order González–Schlegel integration method.^{32,33}

Each stationary structure was characterized as a minimum or a saddle point of index one by a frequency calculation, which also provides thermodynamic quantities such as entropy and zero-point vibrational energy (ZPVE),³⁴ and consequently the rate constant and the preexponential factor of the Arrhenius expression can be estimated. The calculated harmonic vibrational frequencies are overestimated (about 10%) when computed at the HF-SCF level, due to a combination of the neglect of electron correlation and vibrational anharmonicity effects.^{35,36} Thus, the results concerning PM3, AM1, and HF/6-31G** levels were uniformly scaled by a factor of 0.91.³⁷ On the other hand, even if electron correlation is taken into account, the scaling of the frequencies can produce results in better agreement with experiment in some cases.³⁵ In order to study the effect of the scaling at MP2/6-31G**, MP2/6-31++G**, CISD/6-31G**, BLYP/6-31G**, and CASSCF(6,6)/6-31G** levels, we have calculated the corresponding thermodynamic and kinetic parameters either scaling the harmonic frequencies by the same scale factor or not scaling it.

Scaled or unscaled vibrational frequencies below 500 cm^{-1} were treated as classical rotations in computing the vibrational energy, *i.e.*, $E_{\text{vib}} = RT/2$. The imaginary frequency for the TSs was ignored in all calculations. Temperature corrections and absolute entropies were obtained assuming ideal gas behavior, from the scaled or unscaled harmonic frequencies and moments of inertia, by standard methods.^{38,39} The absolute entropies were evaluated by the relation

$$S = S_{\text{tr}} + S_{\text{rot}} + S_{\text{vib}} - R \ln \sigma + R \ln m \quad (3)$$

where S_{tr} , S_{rot} , and S_{vib} are the translational, rotational, and vibrational contributions, respectively, R is the ideal gas constant, σ is the rotational symmetry number,⁴⁰ and m is the multiplicity of the ground state. A standard pressure of 1 atm was taken in the S calculations.

Considerable effort has been devoted to the development of theories to calculate accurately the rate constants for chemical processes.⁴¹ In particular, Truhlar et al.,^{42,43} with their variational transition state theory, Miller et al.,^{44,45} and Rice et al.^{46,47} have developed useful methods to study the reaction dynamics in polyatomic molecular systems. However, the classical transition state theory can still be considered a fairly successful method to describe chemical reactions,^{48,49} and the molecular mechanism of a given chemical reaction can be defined by the TS associated to the chemical interconversion step. We have selected this method to calculate the kinetic parameters in the present study. The rate constant ($k(T)$) for each elementary step of the kinetic scheme (see below) was computed using this theory^{48,50} assuming that the transmission coefficient is equal to 1, as expressed by the following relation:

$$k(T) = (kT/h) \exp(\Delta S^\ddagger/R) \exp(-\Delta E^\ddagger/RT) \quad (4)$$

where ΔE^\ddagger and ΔS^\ddagger are the energy and entropy changes between each reactant and its corresponding transition structure, k is the Boltzmann constant, and h is the Planck constant. ΔE^\ddagger was calculated as follows:

$$\Delta E^\ddagger = V^\ddagger + \Delta ZPVE + \Delta E(T) \quad (5)$$

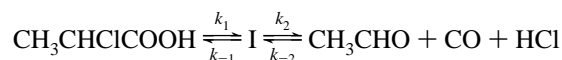
where V^\ddagger is the potential energy barrier at 0 K and $\Delta ZPVE$ and $\Delta E(T)$ are the differences of ZPVEs and temperature corrections between the TS and the corresponding reactants. Finally, the preexponential factor (A) of the Arrhenius expression of the rate constant was calculated by the following relation:

$$A = (kT/h) \exp(\Delta S^\ddagger/R) \quad (6)$$

Results and Discussion

Geometry of the Stationary Structures and the Reaction Pathways. In the study of a chemical reaction, it is important to realize that the finding of one TS does not exclude the possibility of alternative reaction paths having other TSs. In order to discriminate between alternative reaction channels for the molecular mechanism of the decomposition of the 2-chloropropionic acid, an extensive exploration of the PES by means of PM3 and AM1 semiempirical procedures has rendered only two TSs: **TS1** and **TS2**, and three minima: 2-chloropropionic acid (**R**), α -propiolactone intermediate hydrogen bonded to hydrogen chloride (**I**), and acetaldehyde, carbon monoxide, and hydrogen chloride (**P**). The possibility of an heterolytic fragmentation of **R** yielding the chloride anion and the corresponding carbocation has to be discarded because an exhaustive search points out that a saddle point of index one linking **R** with the two ions is not localized on PES. Further calculations have been made in order to obtain the stationary points at higher levels of theory: *ab initio* HF/6-31G**, BLYP/6-31G**, MP2/6-31G**, MP2/6-31++G**, CISD/6-31G**, and CASSCF(6,6)/6-31G**.

The theoretical results agree with the experimental data reported by Chuchani et al.,¹ describing a two-step process:



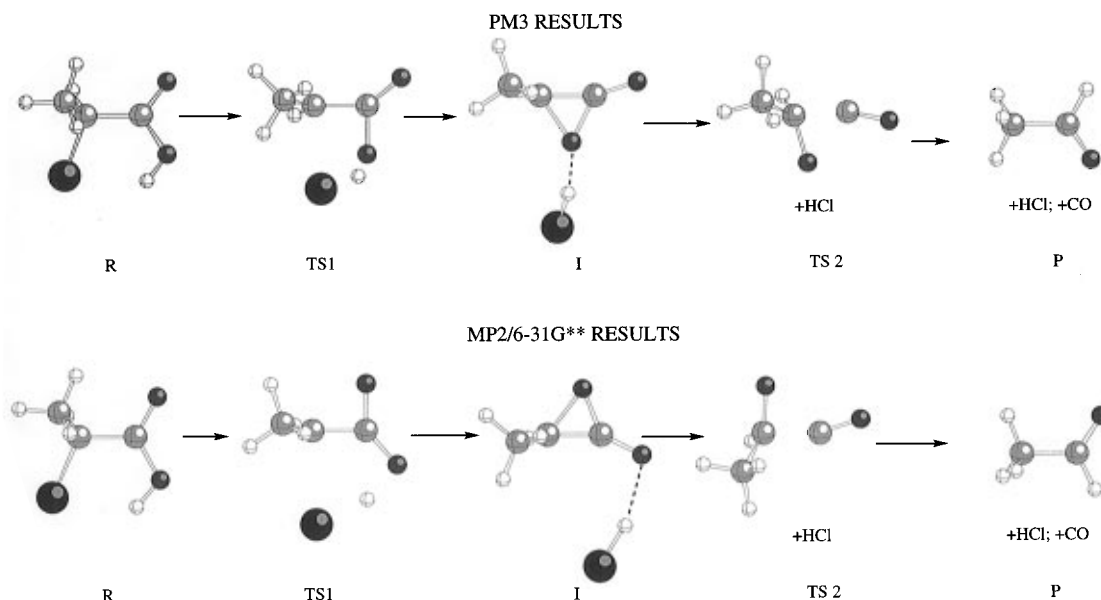


Figure 2. Stationary points found at the PM3 semiempirical level and at the MP2/6-31G** level.

The first step is the formation of the intermediate **I** via the **TS1**. The minimum-energy pathway on the potential energy surface for the decomposition of 2-chloropropionic acid involves initial loss of hydrogen chloride and cyclization to form the **I** ring, followed by the ring opening leading to carbon monoxide and acetaldehyde. The **TS1**, associated with the first step, can be described as a distorted five-membered ring with participation of the leaving chloride and the carboxylic hydrogen. As was originally suggested,¹ this result can be justified due to the different acidity between the H of COOH ($pK_a = 4.8$), which will assist the leaving chloride, and the H of the CH₃ group ($pK_a = 48.0$). The **TS2**, associated with the second step, corresponds to the loss of a CO molecule due to the cleavage of C₁–C₂ and O₁'–C₂ (or O₁–C₂, see later) bonds.

In Figure 2, we show the geometries of the corresponding stationary points found at PM3 and MP2/6-31G** calculation levels. The cyclization to the α -propiolactone appears to be carried out by the hydroxylic oxygen of the carboxyl group when calculation is done with the PM3 method while all other methods show this cyclization to be carried out by the carbonylic oxygen.

A selected set of geometric parameters for **R**, **TS1**, **I**, **TS2**, and **P** are reported as Supporting Information. The completely optimized geometries are available from the authors on request. An analysis of these parameters shows that the geometries of the minima (**R**, **I**, and **P**) are weakly dependent on the computational method. Thus, the discrepancies found for **R** distances and angles are quite low (among the ab initio results, the distances vary less than 0.09 Å and the bond angles less than 6.9°), while the differences found for the selected dihedral angles (mainly due to the free rotation around the C₁–C₂ single bond) are in the range from 3.1° to 19.1°. The dependence on the computational method is more obvious between the ab initio and the semiempirical procedures. Poor dependence of **I** geometry upon computing method can also be seen: the differences found for distances and angles are lower than 0.09 Å and 9.5°, respectively. The PM3 and AM1 semiempirical procedures show dihedral angles rather different from the other methods, which present dihedral angles differing less than 2.7°. The **P** geometry can be considered as invariant; the distances, bond angles, and the dihedral angle vary with respect to the computation method less than 0.043 Å, 1.9°, and 0.2°, respectively.

As expected, TS geometries were found to be quite sensitive to the level of theory used. For **TS1**, ab initio methods yield similar values, but large variations have been detected between the semiempirical and ab initio results. The maximum discrepancies found among ab initio results in the distances, angles and dihedral angles are 0.535 Å, 11.5°, and 10.8°, respectively. The geometric parameters for **TS2** seem to be quite independent of the computational level used, especially the distances: discrepancies lower than 0.061 Å have been found. The bond angles show variations lower than 7.1° and the values for the dihedral angles (with the exception of the PM3 results) vary up to 11.1°.

Transition Vector and Vibrational Frequencies. The imaginary frequency, the force constants for those selected geometric parameters with nonzero components in the TV, and the corresponding components in this control space for **TS1** and **TS2** have also been included as Supporting Information.

The values of the force constants associated to the components of TV for **TS1** are somewhat depending on the calculation level, being the largest value the corresponding to the O₁–C₂–C₁ bond angle in all cases. They are all positive (except the corresponding to the H₁–Cl bond at MP2/6-31G**, yielding a low negative value) and the negative eigenvalue arises from the cross-terms off-diagonal in the force constant matrix. The imaginary frequency values are in a wide range of 223–1140i cm⁻¹. The normal mode analysis of these structures yields a relatively low imaginary frequency, indicating that the **TS1** is associated with the heavy atoms motions.

The values of the components of the TV are not very dependent upon computing level. However, some differences can be sensed between semiempirical and ab initio results: PM3 values are expected to be different, as a result of the commented mechanistic difference and AM1 yields a TV with the dominant contributions of Cl–C₂ bond distance and O₁'–C₁–C₂ bond angle. The ab initio procedures render the Cl–C₂ and H₁–Cl bond distances as well as the O₁'–C₁–C₂ bond angle as the dominant components of TV at all calculation levels. This result confirms that the TSs are well associated to the loss of hydrogen chloride with participation of C₁, C₂, and O₁' atoms, leading to the formation of the α -propiolactone ring.

In order to understand the electronic changes undergone when going from **R** to **TS1**, a Mulliken population analysis has been carried out. There is a displacement of negative charge toward

TABLE 1: Relative Electronic Energies (kJ/mol) to the Reactant (R)^a

	TS1 (ΔE_1)	I	TS2	ΔE_2	P
MP2/6-31G**	216.65	158.36	296.18	137.82	105.52
MP2/6-31++G**	214.14	163.76	289.78	126.02	107.65
CISD/6-31G**	239.70	166.06	317.52	151.46	89.16
CASSCF(6,6)/6-31G**	210.20				

^a Values for **R** energy are as follows: total energy, MP2/6-31G**:
 -726.679 014 au; MP2/6-31++G**:
 -726.701 787 au; CISD/6-31G**:
 -726.513 563 au; CASSCF(6,6)/6-31G**:
 -725.850 546 au. The energetic differences between **TS1** and **R** (ΔE_1) and **TS2** and **I** (ΔE_2) are also indicated.

the Cl atom and the corresponding value is in the range 0.25–0.65 au at **TS1**, depending on the computational level. This fact points out that the **TS1** can be described as a polar five-membered (C₁, C₂, O₁, Cl, and H₁ centers) cyclic structure with participation of the carbonylic oxygen (O₁') of the carboxylic group. The presence of an intimate ion-pair type of intermediate (chloride anion and carbocation structure) along the reaction pathway can be discarded, in agreement with the conclusions obtained from recent experimental data by Chuchani et al.² It must be noted that, according to our theoretical results, except PM3, it is the carbonylic oxygen (O₁') the atom that assists the cyclization, instead of the originally suggested¹ hydroxylic oxygen (O₁).

For **TS2**, the components' weights forming the corresponding TV are also dependent upon computing method. In this case, the different methods used render the following dominant components of the TV: PM3 and AM1 yield O₁–C₂–C₃–H₂ and H₂–C₂–C₁–C₃ dihedral angles, respectively; HF/6-31G** and CISD/6-31G** render C₁–C₂ distance, while MP2/6-31G**, MP2/6-31++G**, and BLYP/6-31G** levels show C₂–C₁–O₁' bond angle as the dominant contribution. Although the dominant components vary, in this case there are several internal variables that always participate significantly in the TV: the C₁–C₂ and O₁–C₂ distances, the C₂–C₁–O₁', C₃–C₂–C₁ and H₂–C₂–C₁ bond angles and the H₂–C₂–C₁–C₃ dihedral angle. These internal coordinates are related with the process of cleavage of the C₁–C₂ bond, the formation of the C₂–O₁ double bond, and the formation of the CO molecule. The values corresponding to the force constants are qualitatively invariant to the calculation level used, being the one associated to O₁'–C₁ internal variable the largest value, in the range 1.03–1.42 au. The force constants are all positive and the negative eigenvalue arises from the cross-terms off-diagonal in the force constants matrix. This fact is similar to the result obtained for **TS1**. The imaginary frequency values are in the range 505–694i cm⁻¹ for **TS2**. The normal mode analysis of these structures yields also a relatively low imaginary frequency, thus indicating that the TS is associated with the heavy atoms motions.

Energetics and the Application of the Transition State Theory. The energetic results for the stationary points obtained with the MP2/6-31G**, MP2/6-31++G**, CISD/6-31G**, and CASSCF(6,6)/6-31G** calculation levels are reported in Table 1 (ZPVE corrections not included). The rest of energetic results are reported as Supporting Information. The global process is endothermic, and the energetic results are markedly dependent upon computing method. The energy barrier for the first step (**R** to **TS1**) calculated by using the semiempirical methods are 339.07 and 277.06 kJ/mol at PM3 and AM1, respectively. The results with ab initio method without correlation diminishes this value to 238.81 kJ/mol, and the inclusion of the correlation energy at MP2/6-31G** level further reduces the energy barrier to 216.65 kJ/mol and at MP2/6-31++G** level to 214.14 kJ/

mol; CISD/6-31G** renders an energy barrier of 239.70 kJ/mol and BLYP/6-31G** of 142.42 kJ/mol. By using the MCSCF method, an energy barrier of 210.20 kJ/mol is obtained.

The values obtained for the barrier height associated with the second step with AM1 and PM3 semiempirical procedures are 79.33 and 87.11 kJ/mol, respectively; with ab initio methods range from 126.02 to 151.46 kJ/mol and with the DFT procedure is 113.34 kJ/mol.

The relative stability of **I** is in the range from 193.51 to 207.07 kJ/mol at semiempirical level while ab initio methods diminishes this value to the range from 155.02 to 166.06 kJ/mol, BLYP/6-31G** method further reduces this value to 136.77 kJ/mol. The DFT procedure yields an energy profile more smooth than the others. This energetic trend has been recently noticed by our group in several studies of different chemical processes (like, for instance, the transposition of the α -chlorocyclobutanone⁵¹ or the decomposition of *N*-chloro- α -amino acids⁵²) and will be reflected in the calculation of thermodynamic and kinetic parameters. This fact points out that, although the geometries of the stationary points and the TV associated to **TSs** are described within the DFT methodology in a similar way than within standard calculation schemes, the energy values obtained must be taken with care and it is not obvious that DFT is appropriate in this respect.

The system under study undergoes a two-consecutive-step process, which can be schematically described as



Two initial assumptions concerning the overall behavior of the system can be done:⁵³

(a) The two steps are essentially irreversible. This assumption can be justified because the two processes are decompositions and the entropy of the system increases along the reaction pathway. The values for the enthalpy, entropy and free energy changes between **R** and **I**, between **I** and **P** and for the whole process are presented in Table 2 and in the Supporting Information. The global process is predicted to be endothermic and nonspontaneous at standard temperature, except at HF/6-31G** level of theory, where a negative value is found for ΔG . If this assumption is proved to be true, then the relevant kinetic data is controlled by a single rate-determining step, which will correspond to the direct step with the smallest rate constant. In all methods used the rate-determining step is the first one, as can be seen from the kinetic results shown in Table 3 and the Supporting Information. The observed first-order rate constant and preexponential factor will coincide with the theoretical k_1 and A_1 , respectively.

(b) The two steps are reversible at any (relevant) extent. Then it should be noted that the intermediate **I** is appreciably less stable (thermodynamically) than either reactants or products, as can be seen from results shown in Tables 1 and 2, and it will behave as a steady state intermediate.⁵⁴ A complete kinetic analysis under the steady state approximation for **I**, assuming that the only starting material is **R**, yields that the observed first-order rate constant would be dependent on the initial amount of **R**. Since this is not the case,¹ this assumption can be discarded. However, it is still possible that one of the two steps could be considered as reversible. For the possibility of a reversible first step we obtain for the direct process the following rate equation:

$$-\frac{d[\text{R}]}{dt} = \frac{k_1 k_2}{k_{-1} + k_2} [\text{R}] \quad (8)$$

TABLE 2: Thermodynamic Parameters (ΔH and ΔG in kJ/mol, ΔS in J/(mol·K)) Obtained for the Process under Study at Standard Pressure (1 atm) and Temperature (298.15 K)^a

	ΔH_1	ΔH_2	ΔH	ΔS_1	ΔS_2	ΔS	ΔG_1	ΔG_2	ΔG
MP2 (a)	139.10	-58.68	80.42	26.35	83.61	109.96	131.24	-83.61	47.63
MP2 (b)	137.42	-59.79	77.64	27.09	81.91	108.99	129.35	-84.21	45.14
MP2++ (a)	144.61	-61.82	82.80	31.53	97.07	128.60	135.21	-90.76	44.46
MP2++ (b)	142.94	-62.91	80.03	34.12	95.38	129.49	132.77	-91.34	41.42
CISD (a)	148.59	-83.05	65.53	62.83	88.54	151.38	129.85	-109.45	20.40
CISD (b)	146.86	-84.25	62.61	62.84	86.64	149.49	128.12	-110.08	18.05

^a The enthalpy, entropy, and free energy changes between **R** and **I** (ΔH_1 , ΔS_1 , and ΔG_1), between **I** and **P** (ΔH_2 , ΔS_2 , and ΔG_2), and for the whole process (ΔH , ΔS , and ΔG) are shown. For MP2 and CISD calculations, the values obtained including a scale factor of 0.91 (a) and without including it (b) are presented.

and an apparent rate constant of $k_1 k_2 / (k_{-1} + k_2)$ will coincide with the observed first-order rate constant. Under this assumption, if $k_{-1} \ll k_2$, the observed first-order rate constant and preexponential factor are equal to k_1 and A_1 , respectively. Conversely, if $k_{-1} \gg k_2$, then the observed first-order rate constant, preexponential factor, and ΔE^\ddagger for the overall process can be obtained through

$$k_{\text{ap}} = \frac{k_1 k_2}{k_{-1}} \quad A_{\text{ap}} = \frac{A_1 A_2}{A_{-1}} \quad \Delta E_{\text{ap}}^\ddagger = \Delta E_1^\ddagger + \Delta E_2^\ddagger - \Delta E_{-1}^\ddagger \quad (9)$$

For the possibility of a reversible second step, we obtain again an observed first-order rate constant and preexponential factor equal to k_1 and A_1 . Thus, we cannot distinguish between a completely irreversible process and a process with an irreversible first step. A theoretical prediction of the rate constant and the preexponential Arrhenius factor may be given by the transition state theory following the above equations.

The PM3 semiempirical procedure renders the results in worst accordance with experimental data (results reported as Supporting Information). In this case, considering the global process as either irreversible or reversible, the kinetic parameters are obtained from the first direct step, and the calculated rate constant (k_1) is much lower than the observed experimental value. This is a consequence of the very high activation energy found for the first step, 321.9 kJ/mol, if compared with the experimental value of 186.9 kJ/mol.¹ The alternative mechanism predicted by this method has to be discarded as a realistic description of the chemical process. The results obtained by means of the use of AM1 semiempirical method render an energy barrier about 39% higher than the experimental value. An appreciable difference for the k and A values is found between the semiempirical results and the experimental data.

By use of the Hartree-Fock method (6-31G** basis set level) without inclusion of correlation energy, the results, although still not very accurate, are much better if we consider the whole process or the first step as essentially irreversible. In this case the calculated activation energy (ΔE_1^\ddagger) is about 19% higher than the experimental value; the preexponential factor (A_1) enters into the experimental range, but the rate constant (k_1) is still between 5 and 8 orders of magnitude lower than the observed value. If the possibility of a reversible first step is taken into account, the results ($\Delta E_{\text{ap}}^\ddagger$, A_{ap} , and k_{ap}) are in worst agreement with the experimental data. These results suggest that the real process is better described as irreversible or as having an irreversible first step.

If electron correlation is included (MP2/6-31G** method) and the process is considered to be irreversible, the predicted energy barrier is 5% higher than the observed one (less than twice the experimental error). Again, the preexponential factor agrees with the experimental data, and the rate constant value is very close to the experimental range. Increasing the size of

the basis set by including diffuse functions, at the MP2/6-31++G** level, we find values in accordance with experiment: the energy barrier is 3.6% higher than the observed value (the experimental error is 2.7%), and the preexponential factor and rate constant enter into the experimental range. The possibility of a reversible process can be discarded due to the large discrepancies obtained for A_{ap} and k_{ap} between theoretical and experimental values. If electron correlation is included at the CISD/6-31G** level, the results for ΔE_1^\ddagger , A_1 , and k_1 are similar to that obtained at the much less expensive HF/6-31G** level. This fact points out that the Moller-Plesset approach at second-order perturbation theory is a better choice than the CISD approach.

At the BLYP/6-31G** level of calculation, the results obtained are not consistent with the experimental data, except for the preexponential factor, which enters into the experimental range for the irreversible assumption. These results point out that this method is unable to correctly describe the decomposition process.

We have also performed a complete geometry optimization at the MCSCF level by means of the CASSCF(6,6)/6-31G** method for **R** and **TS1**, in order to calculate the k_1 rate constant and A_1 Arrhenius preexponential factor. The inclusion of six active electrons is consequence of the total number of bonds that are being broken/formed in the first step of the reaction: the C₂-Cl, O₁-H₁, and double C₁-O₁' bonds are broken while the Cl-H₁, O₁'-C₂, and double C₁-O₁ bonds are formed. The six molecular orbitals included into the active space are chosen to represent at **TS1** the σ -bonding interactions between Cl-H₁ and O₁'-C₂ and the π -bonding interaction between C₁-O₁, as well as the σ -antibonding O₁-H₁, Cl-C₂ and the π -antibonding interaction between C₁-O₁'. Although the A_1 preexponential factor is not correctly reproduced, the result obtained for k_1 is comprised into the experimental range.

Scaling of the Frequencies. We have performed the frequency calculations at PM3, AM1, and HF/6-31G** computation levels, including a factor of 0.91 in order to uniformly scale the calculated harmonic vibrational frequencies. This has been demonstrated to give more reliable results by correcting at a significant extent the neglect of electron correlation and the vibrational anharmonicity effects.³⁵⁻³⁷ However, it is not clear whether at different calculation levels which include electron correlation the uniform scaling of the frequencies improves the results.³⁵ In order to find some insights concerning the convenience of uniformly scaling the frequencies, scaled and unscaled vibrational frequency calculations have been carried out at the MP2, CISD, DFT, and CASSCF methods. The inclusion of the scale factor yields an increment of the enthalpy changes (see Table 2) by up to 4.7%; a reduction in the entropy change corresponding to the first step by up to 7.6%, an increment in the entropy change for the second step by up to 2.2%, and small variations for the total entropy change (up to 1.3%); the free energy changes increase by up to 13%. The

TABLE 3: Theoretically Calculated Values of ΔE^\ddagger (kJ/mol), A (s^{-1} , except A_{-2} , in $L^2 \text{ mol}^{-2} s^{-1}$), and k (s^{-1} , except k_{-2} , in $L^2 \text{ mol}^{-2} s^{-1}$) for the Elementary Steps of the Process under Study and Apparent Values for These Parameters According to the Kinetic Scheme^a

	ΔE^\ddagger_1	A_1	k_1	ΔE^\ddagger_{-1}	A_{-1}	k_{-1}	ΔE^\ddagger_2	A_2	k_2	ΔE^\ddagger_{-2}	A_{-2}	k_{-2}	$\Delta E^\ddagger_{\text{up}}$	A_{up}	k_{up}
MP2 (a)	198.3	2.87×10^{12}	5.29×10^{-23}	59.2	1.21×10^{11}	5.20×10^0	131.5	7.65×10^{12}	7.12×10^{-11}	190.1	3.28×10^8	1.60×10^{-25}	270.6	1.82×10^{14}	7.24×10^{-34}
MP2 (b)	196.4	2.87×10^{12}	1.10×10^{-22}	59.0	1.10×10^{11}	5.05×10^0	130.9	7.71×10^{12}	9.16×10^{-11}	190.6	4.06×10^8	1.62×10^{-25}	268.3	2.01×10^{14}	2.00×10^{-33}
MP2++ (a)	195.5	5.23×10^{12}	2.96×10^{-22}	50.9	1.18×10^{11}	1.45×10^2	120.0	7.61×10^{12}	7.28×10^{-9}	181.8	6.48×10^7	9.17×10^{-25}	264.6	3.38×10^{14}	1.49×10^{-32}
MP2++ (b)	193.6	5.22×10^{12}	6.25×10^{-22}	50.7	8.62×10^{10}	1.14×10^2	119.4	7.67×10^{12}	9.25×10^{-9}	182.3	8.00×10^7	9.19×10^{-25}	262.3	4.65×10^{14}	5.08×10^{-32}
CISD (a)	223.0	3.92×10^{12}	3.30×10^{-27}	74.5	2.05×10^9	1.85×10^{-4}	144.5	8.71×10^{12}	4.20×10^{-13}	227.6	2.07×10^8	2.81×10^{-32}	293.1	1.67×10^{16}	7.49×10^{-36}
CISD (b)	221.4	3.97×10^{12}	6.41×10^{-27}	74.6	2.07×10^9	1.79×10^{-4}	143.8	8.60×10^{12}	5.53×10^{-13}	228.0	2.56×10^8	2.87×10^{-32}	290.7	1.65×10^{16}	1.98×10^{-35}
CAS (a)	199.4	1.07×10^{14}	1.26×10^{-21}												
CAS (b)	198.1	1.01×10^{14}	1.94×10^{-21}												

^a The values of A_{-2} and k_{-2} are reported for the sake of completeness. The results obtained by using a scale factor of 0.91 (a) and without using it (b) are presented. The experimental value for the energy barrier is 186.9 ± 5.1 kJ/mol, for the preexponential factor is in the interval between $A = 1.26 \times 10^{12}$ and $A = 9.12 \times 10^{12}$ (s^{-1}) and for the rate constant between $k = 2.944 \times 10^{-22}$ and $k = 1.305 \times 10^{-19}$ (s^{-1}) at 298.15 K.

endothermic and nonspontaneous character of the whole process is somewhat increased when the scale factor is included to obtain the vibrational frequencies.

At the MP2/6-31G** level, the inclusion of the scale factor renders worst results (see Table 3): the energy barrier (ΔE^\ddagger_1) is even increased, and consequently the rate constant (k_1) is reduced and does not enter into the experimental range, although the preexponential factor (A_1) is not significantly affected. The same trend is found at the rest of computing levels tested, although in the MP2/6-31++G** and CASSCF(6,6) cases the rate constant enters into the experimental range either scaling or not scaling the frequencies, and in the BLYP and CISD cases the rate constant does not enter the experimental range neither scaling nor not scaling the frequencies. Thus, the possibility of uniformly scaling the frequency values at these calculation levels is not recommended.

Conclusions

The reaction pathway for the unimolecular decomposition of the 2-chloropropionic acid in the gas phase has been investigated. The stationary points (**R**, **TS1**, **I**, **TS2**, and **P**) were localized and characterized by using PM3 and AM1 semiempirical procedures, the Hartree–Fock method at the 6-31G** basis set level, and BLYP/6-31G** within the density functional theory. The correlation effects were also included by using the perturbational approach at the MP2/6-31G** and MP2/6-31++G** levels, the variational approach at the CISD/6-31G** level, and by means of a MCSCF approach in the (6,6) active space with the 6-31G** basis set. Some important features were clarified, and the results can be summarized as follows:

(1) The minimum-energy pathway on the potential energy surface for the decomposition of 2-chloropropionic acid involves the loss of hydrogen chloride with initial cyclization to an α -propiolactone intermediate, followed by a ring opening leading to carbon monoxide and acetaldehyde.

(2) The first transition structure, associated with the formation of the α -propiolactone intermediate, can be described as a polar five-membered cyclic structure with participation of the carbonylic oxygen of the carboxyl group. The second step corresponds to an opening of the oxirane ring with formation of carbon monoxide and acetaldehyde molecules.

(3) The semiempirical PM3 procedure renders that the formation of the α -propiolactone intermediate is made with the help of the hydroxylic oxygen of the carboxyl group while the other theoretical methods point out this cyclization to occur by using the carbonylic oxygen of the carboxyl group.

(4) The validity of the theoretical results is confronted with the experimental data, by comparing the rate constant and the Arrhenius preexponential factor calculated within the transition state theory. Good agreement with the experimental values is found when the irreversible character of the first step is considered, and the formation of the α -propiolactone intermediate is the rate-limiting step of the global process. In this sense, the alternative mechanism predicted by the PM3 method can be discarded. The rate constant values obtained with AM1, HF, and CISD methods are lower than the experimental data; meanwhile, the BLYP procedure gives a much higher value. It is necessary to include the correlation energy at the MP2 level or to use a MCSCF procedure to obtain accurate values for the rate constants.

(5) While it is well established that the use of scaled vibrational frequencies at SCF level of theory without inclusion of the correlation energy improves the results, the use of uniformly scaled vibrational frequencies at MP2, CISD, BLYP, and MCCSF impairs the calculated kinetic parameters for the studied reaction.

We believe that the results presented in this work point out important features of the elimination kinetics of the 2-chloropropionic acid that should be preserved in the characterization of the decomposition processes for related carboxylic acids. This study is now under process and will be presented elsewhere.

Acknowledgment. This work was supported by research funds of the Ministerio de Educación y Ciencia of the Spanish Government by DGICYT (Project PB93-0661). We are very grateful to Prof. G. Chuchani for suggesting this study, providing us their extensive experimental work on decomposition processes, and for the helpful discussions maintained when preparing the manuscript. All calculations were performed on an IBM RS6000 workstation of the Departament de Ciències Experimentals of the Universitat Jaume I, on a cluster of Hewlett-Packard 730 workstations and on two Silicon Graphics Power Challenge L of the Servei d'Informàtica of the same University. We are most indebted to these centers for providing us with computer capabilities.

Supporting Information Available: Tables giving the main geometric parameters for **R**, **I**, and **P**; the imaginary frequency, main components of TV, corresponding geometric parameters and force constants for **TS1** and **TS2**, and energetic, thermodynamic, and kinetic parameters (9 pages). Ordering information is given on any current masterhead page.

References and Notes

- Chuchani, G.; Rotinov, A. *Int. J. Chem. Kinet.* **1989**, *21*, 367.
- Chuchani, G.; Domínguez, R. M.; Rotinov, A. *Int. J. Chem. Kinet.* **1991**, *23*, 779.
- Chuchani, G.; Martín, I.; Rotinov, A.; Domínguez, R. M. *J. Phys. Org. Chem.* **1993**, *6*, 54.
- Chuchani, G.; Martín, I.; Rotinov, A.; Domínguez, R. M.; Pérez I., M. *J. Phys. Org. Chem.* **1995**, *8*, 133.
- Chuchani, G.; Domínguez, R. M. *Int. J. Chem. Kinet.* **1995**, *27*, 85.
- Frisch, M. J.; Trucks, G. W.; Schlegel, H. B.; Gill, P. M. W.; Johnson, B. G.; Wong, M. W.; Foresman, J. B.; Robb, M. A.; Head-Gordon, M.; Replogle, E. S.; Gomperts, R.; Andres, J. L.; Raghavachari, K.; Binkley, J. S.; Gonzalez, C.; Martin, R. L.; Fox, D. J.; Defrees, D. J.; Baker, J.; Stewart, J. J. P.; Pople, J. A. *GAUSSIAN92/DFT, Revision G.4*; Gaussian Inc.: Pittsburgh, PA, 1993.
- Frisch, M. J.; Trucks, G. W.; Schlegel, H. B.; Gill, P. M. W.; Johnson, B. G.; Robb, M. A.; Cheeseman, J. R.; Keith, T.; Peterson, G. A.; Montgomery, J. A.; Raghavachari, K.; Al-Laham, M. A.; Zakrzewski, V. G.; Ortiz, J. V.; Foresman, J. B.; Cioslowski, J.; Stefanov, B. B.; Nanayakkara, A.; Challacombe, M.; Peng, C. Y.; Ayala, P. Y.; Chen, W.; Wong, M. W.; Andres, J. L.; Replogle, E. S.; Gomperts, R.; Martin, R. L.; Fox, D. J.; Binkley, J. S.; Defrees, D. J.; Baker, J.; Stewart, J. J. P.; Head-Gordon, M.; Gonzalez, C.; Pople, J. A. *GAUSSIAN94, Revision B.1*; Gaussian, Inc.: Pittsburgh, PA, 1995.
- Stewart, J. J. P. *J. Comput. Chem.* **1989**, *10*, 209.
- Stewart, J. J. P. *J. Comput. Chem.* **1989**, *10*, 221.
- Dewar, M. J. S.; Zoebisch, E. G.; Healy, E. F.; Stewart, J. J. P. *J. Am. Chem. Soc.* **1985**, *107*, 3902.
- Frisch, M. J.; Pople, J. A.; Binkley, J. S. *J. Chem. Phys.* **1984**, *80*, 3265.
- Moller, C.; Plesset, M. S. *Phys. Rev.* **1934**, *46*, 618.
- Clark, T.; Chandrasekhar, J.; Spitznagel, G. W.; Schleyer, P. v. R. *J. Comput. Chem.* **1983**, *4*, 294.
- Pople, J. A.; Binkley, J. S.; Seeger, R. *Int. J. Quantum Chem. Symp.* **1976**, *10*, 1.
- Hohenberg, P.; Kohn, W. *Phys. Rev.* **1964**, *136*, B864-B871.
- Kohn, W.; Sham, L. J. *Phys. Rev.* **1965**, *140*, A1133-A1138.
- The Challenge of d and f Electrons*; Salahub, D. R., Zerner, M. C., Eds.; American Chemical Society: Washington, DC, 1989.
- Parr, R. G.; Yang, W. *Density-Functional Theory of Atoms and Molecules*; Oxford University Press: Oxford, 1989.
- Becke, A. D. *Phys. Rev. A* **1988**, *38*, 3098.
- Lee, C.; Yang, W.; Parr, R. G. *Phys. Rev. B* **1988**, *37*, 785-789.
- Miehlich, B.; Savin, A.; Stoll, H.; Preuss, H. *Chem. Phys. Lett.* **1989**, *157*, 200.
- Hegarty, D.; Robb, M. A. *Mol. Phys.* **1979**, *38*, 1795.
- Eade, R. H. E.; Robb, M. A. *Chem. Phys. Lett.* **1981**, *83*, 362.
- Schlegel, H. B.; Robb, M. A. *Chem. Phys. Lett.* **1982**, *93*, 43.
- Bernardi, F.; Bottini, A.; McDougall, J. J. W.; Robb, M. A.; Schlegel, H. B. *Faraday Symp. Chem. Soc.* **1984**, *19*, 137.
- Frisch, M. J.; Ragazos, I. N.; Robb, M. A.; Schlegel, H. B. *Chem. Phys. Lett.* **1992**, *189*, 524.
- Schlegel, H. B. *J. Comput. Chem.* **1982**, *3*, 214.
- Schlegel, H. B. *J. Chem. Phys.* **1982**, *77*, 3676.
- Tsai, C. J.; Jordan, K. D. *J. Phys. Chem.* **1993**, *97*, 11227.
- Stanton, R. W.; McIver Jr., J. V. *J. Am. Chem. Soc.* **1975**, *97*, 3632.
- Fukui, K. *J. Phys. Chem.* **1970**, *74*, 4161.
- González, C.; Schlegel, H. B. *J. Phys. Chem.* **1990**, *94*, 5523.
- González, C.; Schlegel, H. B. *J. Chem. Phys.* **1991**, *95*, 5853.
- Hehre, W. J.; Radom, L.; Schleyer, P. v. R.; Pople, J. A. *Ab Initio Molecular Orbital Theory*; John Wiley & Sons: New York, 1986.
- DeFrees, D. J.; McLean, A. D. *J. Chem. Phys.* **1985**, *82*, 333.
- Curtiss, L. A.; Raghavachari, K.; Trucks, G. W.; Pople, J. A. *J. Chem. Phys.* **1991**, *94*, 7221.
- Grev, R. S.; Janssen, C. L.; Schaefer III, H. F. *J. Chem. Phys.* **1991**, *95*, 5128.
- McQuarrie, D. *Statistical Mechanics*; Harper & Row: New York, 1986.
- Olivella, S.; Solé, A.; García-Raso, A. *J. Phys. Chem.* **1995**, *99*, 10549.
- Herzberg, G. *Molecular Spectra and Molecular Structure*; Van Nostrand: Princeton, NJ, 1945; Vol. 2, pp 508.
- Heidrich, D.; Kliesch, W.; Quapp, W. *Properties of Chemically Interesting Potential Energy Surfaces*; Springer-Verlag: New York, 1991.
- Truhlar, D. G.; Garrett, B. C. *Acc. Chem. Res.* **1980**, *13*, 440.
- Truhlar, D. G.; Isaacson, A. D.; Garrett, B. *Theory of Chemical Reaction Dynamics*; Chemical Rubber Co.: Boca Raton, FL, 1985.
- Miller, W. H.; Schwartz, S.; Tromp, J. W. *J. Chem. Phys.* **1983**, *79*, 4889.
- Miller, W. H. *Acc. Chem. Res.* **1993**, *26*, 174.
- Tang, H.; Jang, S.; Zhao, M.; Rice, S. A. *J. Chem. Phys.* **1994**, *101*, 1.
- Rice, S. A.; Jang, S.; Zhao, M. *J. Phys. Chem.* **1996**, *100*, 11893.
- Glasstone, K. J.; Laidler, K. J.; Eyring, H. *The Theory of Rate Processes*; McGraw-Hill: New York, 1941.
- Laidler, K. J. *Theories of Chemical Reaction Rates*; McGraw-Hill: New York, 1969.
- Benson, S. W. *The Foundations of Chemical Kinetics*; McGraw-Hill: New York, 1960.
- Moliner, V.; Castillo, R.; Safont, V. S.; Oliva, M.; Bohm, S.; Tuñón, I.; Andrés, J. *J. Am. Chem. Soc.*, in press.
- Queralt, J. J.; Safont, V. S.; Moliner, V.; Andrés, J. *Theor. Chim. Acta* **1996**, *94*, 247-256.
- Murdoch, J. R. *J. Chem. Educ.* **1981**, *58*, 32-36.
- Frost, A. A.; Pearson, R. G. *Kinetics and Mechanism*, 2nd ed.; John Wiley and Sons: New York, 1961.